NATIONAL ADVISORY COMMITTEE FOR AERONAUTICS

TECHNICAL NOTE 4356

EFFECTS OF COMPRESSIBILITY ON ROTOR HOVERING PERFORMANCE AND SYNTHESIZED BLADE-SECTION CHARACTERISTICS DERIVED FROM MEASURED ROTOR PERFORMANCE OF BLADES HAVING NACA 0015 AIRFOIL TIP SECTIONS

By James P. Shivers and Paul J. Carpenter

Langley Aeronautical Laboratory
Langley Field, Va.

Washington

September 1958

M

NATIONAL ADVISORY COMMITTEE FOR AERONAUTICS

TECHNICAL NOTE 4356

EFFECTS OF COMPRESSIBILITY ON ROTOR HOVERING PERFORMANCE AND SYNTHESIZED BLADE-SECTION CHARACTERISTICS DERIVED FROM MEASURED ROTOR PERFORMANCE OF BLADES HAVING NACA 0015 AIRFOIL TIP SECTIONS

By James P. Shivers and Paul J. Carpenter

SUMMARY

An investigation has been conducted at the Langley helicopter test tower to determine the low tip Mach number blade maximum mean lift coefficients and the high tip Mach number effects of compressibility for rotor blades having NACA 0015 tip airfoil sections. The low tip Mach number rotor-blade maximum mean lift coefficients of a blade having NACA 0015 tip airfoil sections was 1.15, as compared with 1.13 and 1.07 obtained previously with rotors having NACA 63_2-015 and NACA 23015 airfoil sections, respectively. At a higher tip Mach number of 0.70 the rotor having an NACA 0015 tip airfoil section encountered compressibility drag losses at a rotor-blade mean lift coefficient of 0.36, as compared with 0.50 and 0.33 for rotors having NACA 63_2-015 and NACA 23015 airfoil sections, respectively. The comparison of synthesized section characteristics with two-dimensional data obtained previously indicated that the synthesized maximum section lift coefficients were higher than those for the two-dimensional data by about 15 percent at a Mach number of 0.30 and about 10 percent higher at a Mach number of 0.60, and at high Mach numbers the rate of drag rise past drag divergence was less than that shown by two-dimensional data.

The characteristics of the rotor used in the present investigation indicate trends similar to those reported in previous high tip Mach number investigations; that is, at low Mach numbers there is a stable (nose-down) pitching moment past rotor-blade drag divergence, the Mach number for rotor-blade drag divergence is higher than that indicated by two-dimensional data, and increases in tip Mach number lower the maximum efficiency of the rotor as defined by its figure of merit.

INTRODUCTION

One method of meeting the requirements of increased helicopter speeds and higher disk loadings is to increase the rotor-blade tip Mach number. Design studies of helicopters with rotor tip Mach numbers in the high subsonic range and with high blade loadings have emphasized the need for experimental rotor performance and blade pitching-moment data.

This investigation is a continuation of a general research program (refs. 1 to 4) to determine the low tip Mach number stall and high tip Mach number compressibility effects on rotors having various NACA airfoil sections as the primary variable. Although these data are limited to hovering, the onset and rate of growth of the stall and compressibility effects can be analyzed to provide guidance in the selection of airfoil sections for rotors operating at high tip speeds and high tip-speed ratios. In addition, the measured rotor hovering performance can be used to synthesize rotor airfoil section lift and drag characteristics. It is suggested that these synthesized data might be used in calculating helicopter forward-flight performance (ref. 5). However, it should be pointed out that the validity of this procedure has not been checked experimentally and can only be considered tentative at this time. The present investigation extends the program to include a rotor having an NACA 0015 airfoil section at the blade tip.

The rotor blades were tested on the Langley helicopter test tower, and results of the hovering performance are presented for a tip Mach number range from 0.27 to 0.81 (disk loadings up to 5.85 pounds per square foot) and for a corresponding blade-tip Reynolds number range from 1.64×10^6 to 4.78×10^6. In addition, synthesized rotor airfoil section lift and drag characteristics derived from the measured hovering performance are presented and compared with two-dimensional section data obtained previously. The rotor low tip Mach number maximum lift and high tip Mach number compressibility effects are discussed and compared with those of rotors having 15-percent-thick tip airfoil sections (refs. 1 and 2).

SYMBOLS

a straight-line slope of section lift coefficient against section angle of attack, c_l/α_r, radians (assumed to be 5.73 for incompressible calculations)

number of blades

C_m rotor-blade pitching-moment coefficient, $\frac{M_Y}{R\frac{\rho}{2}(\Omega R)^2 c_e^2}$

C_Q rotor torque coefficient, $\frac{Q}{\pi R^2 \rho (\Omega R)^2 R}$

$C_{Q,o}$ rotor profile-drag torque coefficient, $\frac{Q_o}{\pi R^2 \rho (\Omega R)^2 R}$

C_T rotor thrust coefficient, $\frac{T}{\pi R^2 \rho (\Omega R)^2}$

c blade chord at radius r, ft

$c_{d,o}$ airfoil section profile-drag coefficient

c_e equivalent blade chord, $\frac{\int_0^R cr^2 dr}{\int_0^R r^2 dr}$, ft

c_l rotor-blade lift coefficient

$\overline{c_l}$ rotor-blade mean lift coefficient, $\frac{6C_T}{\sigma}$

c_t blade chord at tip

M Mach number

M_t rotor-blade-tip Mach number

M_Y rotor-blade pitching moment (about 19.35 percent root chord), lb-ft

N_{Re} Reynolds number at blade tip, $\frac{\rho \Omega R c_t}{\mu}$

Q rotor torque, lb-ft

Q_o rotor profile-drag torque, lb-ft

R	rotor-blade radius, ft
r	radial distance to a blade element, ft
T	rotor thrust, lb
t	maximum blade thickness at radius r, ft
α	airfoil-section angle of attack, deg
α_r	blade-section angle of attack, deg or radians
θ	blade-section pitch angle measured from line of zero lift, deg
θ_1	difference between hub and tip pitch angles, positive when tip angle is larger, radians
μ	coefficient of viscosity, slugs/ft-sec
ρ	mass density of air, slugs/cu ft
σ	rotor solidity, $\frac{bc_e}{\pi R}$
Ω	rotor angular velocity, radians/sec

The figure of merit is equal to $0.707 \frac{C_T^{3/2}}{C_Q}$.

APPARATUS AND TEST METHODS

Rotor Blades

The rotor used for this investigation was a fully articulated, two-blade rotor with flapping hinge located on the center line of rotation and the drag hinge located 12 inches outboard of the center line. The vertical distance between the ground and a horizontal plane through the center of the rotor was 42 feet.

A sketch of the rotor blade with pertinent dimensions is shown in figure 1. The rotor blades were of all metal construction. The radius of the blade from the center line of rotation was 18.84 feet and the rotor solidity was 0.033. The blade had a root chord (measured at 0.14R) of 1.145 feet and tapered linearly to a chord of 0.854 foot at the tip. The blade also had 5.5° of linear washout (tip pitch lower than root pitch).

The blade had an NACA 0015 airfoil section at the tip and tapered to an 11.5-percent-thick airfoil section at the root. The main spar consisted of a leading-edge D-section having a constant chord of 3.2 inches and true NACA 0015 airfoil-section ordinates throughout the entire blade span. The decrease in thickness ratio from 15 percent at the tip to 11.5 percent at the root is caused by an increase in the chord length of the airfoil root section while the physical thickness remains the same as that of the tip section. The thickness distribution of the blade is shown in figure 1. The tip (at 0.98R) of the rotor blade rearward of the 30-percent-chord line deviated from the true airfoil shape by as much as ±0.015 inch; however, the surface of the entire blade was smooth and fair. The smooth blade referred to herein had an 8-inch-wide 0.010-inch-thick vinyl plastic adhesive abrasion strip covering the leading edge. Tests were made with and without the strip in place, and no distinguishable difference in rotor performance was observed.

Test Methods and Accuracy

The procedure used for testing was to set given rotor-blade collective pitch angles and then to vary the rotor speed through a range of tip Mach numbers from minimum operating speed to the maximum allowable because of structural limitations. At each pitch setting data were recorded both from visual dial readings and by an oscillograph. Quantities measured were rotor thrust, rotor torque, blade pitch angle, blade drag angle, blade pitching moment, rotor-shaft rotational speed, and blade flapping angle. The range of test conditions was chosen to determine the low tip Mach number rotor maximum thrust and to exceed the high tip Mach number drag divergence.

In order to study the low-speed stall characteristics, three rows of black nylon tufts were attached to one rotor blade. The rows of tufts were placed at about the 10-, 40-, and 80-percent chordwise stations and were staggered spanwise about 2 inches from the tuft immediately forward. A high-speed motion-picture camera was mounted on the rotor head to record the flow patterns at the maximum rotor lift conditions.

Since rotor blades may develop roughness in field service, a portion of the tests were repeated with a roughness as described in reference 6 applied to the blades. The roughness consisted of 0.011-inch-diameter carborundum particles applied over a surface length corresponding to 8 percent of the chord back from the leading edge on the upper and lower surfaces. The particles covered from 5 to 10 percent of this area. This leading-edge roughness was more severe than is likely to be encountered in practice and was used only to demonstrate an extreme condition.

The estimated accuracies of the basic quantities measured during the tests were as follows: rotor thrust, ±20 pounds; rotor torque, ±50 pound-feet; rotor rotational speed, ±1 revolution per minute; and all angular measurements, ±0.2°. The overall accuracy of the plotted results is believed to be within ±3 percent. For example, at a rotor-blade mean lift coefficient $\overline{c_l}$ of 0.629 ($C_T = 0.0034$) and a tip Mach number of 0.68, the accuracy of the plotted data based on repeatability was about 2 percent for the thrust value of 5,411 pounds, 1.8 percent for the torque value of 6,270 pound-feet, and 0.25 percent for the value of rotational speed of 387 revolutions per minute. All data have been corrected to zero wind velocities. (See ref. 4.)

METHOD OF ANALYSIS

References 1 to 4 indicate that the principal effect of compressibility is a rapid increase in profile-drag torque once the critical combination of tip Mach number and tip angle of attack is exceeded.

A convenient reference for the rate of growth of profile torque losses is the ratio of the profile-drag torque coefficient derived from the test results to that calculated by using both conventional strip analysis and incompressible drag coefficients. (See ref. 7.) The calculated rotor-performance curve is based on a linear lift-coefficient slope $c_l = 5.73\alpha_r$ and on the commonly used drag polar $c_{d,o} = 0.0087 - 0.0216\alpha_r + 0.400\alpha_r^2$ (ref. 8). Since reference 7 does not allow for any tip loss, a 3-percent tip-loss factor (outer 3 percent of the blade produces no lift but has profile drag) was used in the calculations.

The synthesized lift and drag coefficients were obtained by using the method outlined in reference 5. Briefly, this method involves an iteration process in which the section lift and drag characteristics are successively assumed until the results of calculated rotor performance are in agreement with the test measurement.

Pitching-moment coefficients about the feathering axis (19.35 percent chord at 0.14R) derived from the force measured in the rotor-blade pitch-control linkage are presented. The coefficients thus include the contribution of both aerodynamic and mass forces. In this respect, it should be noted that the absence of abrupt changes in the pitching-moment coefficient is of more significance than the actual values.

RESULTS AND DISCUSSION

The measured and calculated rotor hovering performances are presented and compared. The synthesized rotor-blade section data are presented and compared with two-dimensional section data previously obtained. Data are also presented for measured blade pitching moments, rotor efficiency, and rotor compressibility drag rise. A comparison of rotor drag divergence with that shown from the two-dimensional data is also included.

Hovering Performance

Smooth blades.- The hovering performance of the smooth blades is shown in figure 2 as thrust coefficient against torque coefficient for blade-tip Mach numbers of 0.27 to 0.81. A calculated rotor-performance curve based on the assumptions discussed in the methods of analysis is also plotted for comparison.

In general, the experimental low tip Mach number curves (M_t = 0.27 or M_t = 0.37) show good agreement with the calculated curve up to a rotor thrust coefficient of about 0.0050 ($\overline{c_l}$ = 0.918). The maximum rotor-blade mean lift coefficient $\overline{c_l}$ for the present rotor is 1.15 (C_T = 0.00627). This compares with a maximum $\overline{c_l}$ of 1.13 obtained with a rotor having an NACA 63_2-015 airfoil section (ref. 2) and 1.07 for a rotor having an NACA 23015 airfoil section (ref. 1). It might be expected, on the basis of two-dimensional section characteristics, that the rotor having the NACA 23015 airfoil section would have a higher maximum lift than the rotors having NACA 63_2-015 or NACA 0015 airfoil sections. The reasons for the apparently low maximum lift exhibited by the NACA 23015 rotor of reference 1 is not fully understood; however, it is felt that in this instance differences in surface condition and manufacturing tolerance between the rotors might mask the effect of the airfoil section.

The effect of compressibility is characterized by a progressively earlier digression of the rotor performance curve from the calculated incompressible-flow curve as tip Mach number is increased. At the highest tip Mach number of 0.81, the compressibility drag increase is present even at zero thrust (about 20 percent greater profile drag than for the incompressible case).

Rotor efficiency.- The efficiency of the rotor (figure of merit) as a function of tip Mach number and rotor-blade mean lift coefficient for the smooth rotor blades is shown in figure 3. The maximum low tip Mach number (0.27 to 0.46) figure of merit was about 0.74. As tip Mach number was increased, rotor efficiency decreased because of compressibility profile-drag losses. At a tip Mach number of 0.73, the maximum figure of merit was reduced to 0.58.

Effect of tip Mach number on rotor thrust coefficient.- The effect of blade-tip Mach number on rotor thrust coefficient is shown in figure 4. A calculated curve based on a lift-curve slope of 5.73 radians (which is the value commonly used at low tip Mach numbers) is also presented. The experimental thrust values for a given blade pitch angle are higher, in most cases, than those for the calculated curve; therefore, it is indicated that the lift-curve slope is greater than 5.73 radians.

Leading-edge roughness.- A comparison of the performance of rotors with smooth and rough leading edges and with approximate values of M_t of 0.27, 0.46, 0.55, and 0.76 is shown in figure 5. The addition of leading-edge roughness increased the zero-thrust profile torque coefficient by about 50 percent. Also, the maximum rotor-blade thrust coefficient with leading-edge roughness added was reduced about 23 percent at $M_t = 0.27$ and about 10 percent at $M_t = 0.55$.

Generally, leading-edge roughness decreases the rotor-blade mean lift coefficient for drag rise, especially at the lower tip Mach number where the reduction is on the order of 20 percent compared with the value obtained with the smooth blades.

Synthesized Rotor-Blade Section Characteristics

Lift coefficients.- Variation of synthesized section lift coefficients with angle of attack at various Mach numbers obtained from the smooth rotor having an NACA 0015 tip airfoil section are presented in figure 6. The curves have been extended beyond the blade angle of attack for which there were experimental rotor data. The extrapolations, based on previous experience, are shown dashed to indicate their provisional nature. The curves for Mach numbers of 0.1 and 0.2 also are based on previous experience and are synthesized in the same manner as those for the higher Mach numbers.

A comparison of the synthesized data with two-dimensional lift-coefficient data obtained from reference 9 is presented in figure 7. It is seen that in the low Mach number range ($M_t = 0.30$ to 0.60) the synthesized data have higher lift-curve slopes and higher maximum section lift coefficients than those obtained from two-dimensional section data. The maximum lift coefficient ranged from about 15 percent greater than for the two-dimensional data at $M_t = 0.30$ to about 10 percent greater at $M_t = 0.60$. Above $M_t = 0.65$ the synthesized section lift-curve slope was somewhat lower than for the two-dimensional data.

Drag coefficients.- Figure 8 presents the synthesized blade-section drag-coefficient data as a function of Mach number and angle of attack. The incremental increase in drag coefficient caused by operating 0.1 Mach number past drag divergence (where drag divergence is defined as a point where $\Delta c_{d,o}/\Delta M = 0.1$) varies from about 0.038 at angles of attack of 2° and 4° to about 0.022 at angles of attack of 8° and 10°.

A comparison of the synthesized rotor-blade section profile-drag coefficients and the two-dimensional data obtained from reference 9 is presented in figure 9. The Mach numbers for drag divergence are about the same (within 0.03) for the two sets of data.

In general, the synthesized profile-drag coefficients are larger than those shown by the two-dimensional data at Mach numbers below the force break and increase at a lower rate with Mach number above the force break. This trend has been noted before (refs. 2 and 5) and is probably caused by the drag-alleviating effects of the three-dimensional flow around the blade tips.

Rotor-Blade Pitching Moments

Rotor-blade pitching-moment data were obtained for the rotor in the smooth condition and with leading-edge roughness added.

Smooth blades.- In figure 10(a) the effect of tip Mach number on the rotor-blade pitching moments is presented as a plot of measured rotor-blade pitching-moment coefficient against rotor thrust coefficient for the smooth configuration. The pitching-moment data show the same general trends as reported for previous tests (refs. 1, 2, and 4). At low tip Mach numbers there is a stable (nose-down) pitching moment due to a rearward shift in center of pressure as the airfoil approaches maximum lift. At high tip Mach numbers, a stable shift is also seen, probably because of the rearward center-of-pressure shift associated with compressibility effects. The points for drag divergence are noted by ticks on the pitching-moment curves. The pitching moments show a progressively increased nose-down tendency past drag divergence but do not have a definite reversal such as was noted from a previous 15-percent-airfoil test (ref. 2).

Leading-edge roughness.- The effect of leading-edge roughness on the rotor-blade pitching moments is presented in figure 10(b). The rotor blades with leading-edge roughness have pitching-moment trends similar to those shown for the smooth blades. At low tip Mach numbers the principal difference is a reduction of the nose-down moment, which indicates that the center of pressure is slightly farther forward than for the smooth blades. This same effect was noted in the previous tests of a rotor having NACA 63_2-015 airfoil sections (ref. 2). At the highest Mach numbers (0.75 and 0.78) moments are slightly negative compared with the slight positive values for the smooth blades. It should be pointed out that the absolute values of C_m are of little importance and that the main factor is the absence of abrupt changes in pitching-moment slopes.

Rotor-Blade Profile-Drag Torque

The principal effect of compressibility and stall on rotor performance is an increase in the rotor profile-drag torque (refs. 1 to 4). The onset and rate of growth of rotor profile-drag-torque rise are presented in figure 11 as a ratio of $(C_{Q,o})_{measured}$ to $(C_{Q,o})_{calculated}$ against calculated rotor-blade-tip angle of attack. The data show that for the low tip Mach numbers ($M_t = 0.27$ and $M_t = 0.37$) no increase in profile-drag torque above that given by the commonly used drag polar is obtained until blade-tip angles of attack of about 9.0° to 9.5° are reached.

The increase in blade profile drag is associated with the flow separation over the inboard (0.30R to 0.50R) sections of the blade which have calculated section angles of attack 1.0° to 1.5° higher than the tip angle. High-speed motion pictures of tuft patterns have verified the onset of separated flow in this region. At tip angles of attack of 12° to 13°, the profile-drag-torque-ratio curve steepens, and at this point it would be expected that for all practical purposes the entire blade has separated flow.

At tip Mach numbers greater than 0.64 the principal factor influencing the point of drag rise is the tip angle of attack. In general the curves show that the profile-drag torque ratio was approximately doubled for blade-tip angles of attack 2.5° to 3.0° beyond drag divergence.

An alternate method of showing the rotor-blade drag rise and one that is more useful in comparing various rotors is shown in figure 12 as a plot of the profile-drag ratios against rotor-blade mean lift coefficient. At the low tip Mach numbers (0.27 and 0.37) blade mean lift coefficients of 0.95 and 0.92 were obtained before drag divergence. As tip Mach number increases, the $\overline{c_l}$ for drag divergence decreases in much the same manner as the tip angles for drag divergence decrease.

Comparison of Profile-Drag Torque Ratios

A comparison of the profile-drag torque ratios of the present rotor with those obtained from tests of two other rotors having 15-percent-thick tip airfoils (NACA 63_2-015 and NACA 23015) is shown in figure 13 for three representative tip Mach numbers. At $M_t = 0.30$ the rotors having NACA 0015 and NACA 23015 airfoils have about the same $\overline{c_l}$ (0.95) for drag rise. The $\overline{c_l}$ for the rotor having the NACA 63_2-015 airfoil is slightly lower at this particular tip Mach number. This difference is probably not of much significance since, at a slightly higher value of M_t of 0.36, the rotor with an NACA 63_2-015 airfoil (ref. 2) has a $\overline{c_l}$ for drag

divergence equal to that of the rotor with an NACA 0015 airfoil ($\overline{c_l} = 0.96$). The maximum $\overline{c_l}$ value of the rotors having NACA 0015 and NACA 63_2-015 airfoils is about 10 percent higher than that obtained with the rotor having the NACA 23015 airfoil.

At the intermediate tip Mach number (0.50) the rotors with NACA 0015 and NACA 63_2-015 airfoils have practically identical characteristics; whereas, the rotor with an NACA 23015 airfoil has a considerably lower $\overline{c_l}$ for drag rise. At the highest tip Mach number shown (0.70) the rotor having NACA 0015 tip airfoil sections encountered compressibility drag losses at a $\overline{c_l}$ of 0.36, as compared with 0.33 and 0.50 for rotors having NACA 23015 and NACA 63_2-015 airfoil sections, respectively. It then appears that if rotor blades of 15-percent-thick airfoil sections are required for structural reasons, a considerable delay in the onset of compressibility drag rise can be obtained by using NACA 63_2-015 airfoil sections with relatively insignificant penalty in low tip Mach number stall characteristics.

Comparison of Experimental and Two-Dimensional Drag-Divergence Characteristics

Two-dimensional airfoil-section data are often referred to for an indication of the tip Mach number and angle of attack at which rotor compressibility losses occur. A comparison of the rotor-blade drag-divergence tip Mach number with two-dimensional section data (ref. 9) is shown in figure 14. Two methods of obtaining two-dimensional drag-divergence curves are shown: (1) the point at which $\Delta c_{d,o}/\Delta M = 0.1$, and (2) the point at which the drag coefficient first begins to increase. The second method is more consistent with the manner in which the rotor drag-divergence Mach number is defined. The rotor experimental-data points, denoted by symbols, were obtained from figure 11 and represent the points where each of the curves deviated from unity.

The results are similar to those obtained in previous tests (refs. 3 and 5) and indicate that at low tip angles of attack the rotor can operate at higher tip Mach numbers before drag divergence than the two-dimensional data indicate. This increase in tip Mach number for drag divergence is attributed to the drag-alleviating effects of three-dimensional flow over and around the blade tip.

At the low tip Mach numbers the rotor drag rise occurs at a lower tip angle of attack than indicated by the two-dimensional data. As previously shown (fig. 11), this drag rise should be associated with the inboard section angles of attack where separated flow first occurs. These inboard section angles of attack for separated flow are 10.5° to 11°.

SUMMARY OF RESULTS

The low tip Mach number blade maximum mean lift coefficients and high tip Mach number compressibility effects on a rotor having an NACA 0015 tip airfoil section and 5.5° of negative twist (tip pitch lower than root pitch) have been determined over a tip Mach number range from 0.27 to 0.81. Synthesized section profile-drag and lift characteristics derived from the measured hovering performance of a rotor having an NACA 0015 tip airfoil section are presented and compared with equivalent two-dimensional data. The results of this investigation are as follows:

1. At the low tip Mach number of 0.30 the rotor-blade maximum mean lift coefficient of the rotor having an NACA 0015 tip airfoil section was 1.15, as compared with 1.13 and 1.07 obtained with rotors having NACA 63_2-015 and NACA 23015 airfoil sections, respectively.

2. At a tip Mach number of 0.70 the rotor having an NACA 0015 tip airfoil section encountered compressibility drag losses at a rotor-blade mean lift coefficient of 0.36, as compared with 0.50 and 0.33 for rotors having NACA 63_2-015 and NACA 23015 airfoils, respectively.

3. The comparison of synthesized section characteristics with two-dimensional data obtained previously indicated that the synthesized maximum section lift coefficients were higher than those for the two-dimensional data by about 15 percent at a tip Mach number of 0.30 to about 10 percent at a tip Mach number of 0.60, and at high Mach numbers the rate of drag rise past drag divergence was less than that shown by two-dimensional data.

4. The pitching moments showed a progressively increased nose-down tendency past drag divergence but did not have a reversal as was noted from a previous test of a 15-percent-thick airfoil (NACA TN 3850).

5. The drag-divergence point of the rotor was delayed to higher tip Mach numbers than that indicated by two-dimensional data.

6. The rotor efficiency, expressed as the figure of merit, decreased with an increase in tip Mach number. At tip Mach numbers from 0.27 to 0.46 the maximum figure of merit was 0.74. At a tip Mach number of 0.73, the maximum figure of merit was reduced to 0.58.

Langley Aeronautical Laboratory,
National Advisory Committee for Aeronautics,
Langley Field, Va., July 7, 1958.

REFERENCES

1. Carpenter, Paul J.: Effects of Compressibility on the Performance of Two Full-Scale Helicopter Rotors. NACA Rep. 1078, 1952. (Supersedes NACA TN 2277.)

2. Shivers, James P., and Carpenter, Paul J.: Experimental Investigation on the Langley Helicopter Test Tower of Compressibility Effects on a Rotor Having NACA 63_2-015 Airfoil Sections. NACA TN 3850, 1956.

3. Powell, Robert D., Jr.: Compressibility Effects on a Hovering Helicopter Rotor Having an NACA 0018 Root Airfoil Tapering to an NACA 0012 Tip Airfoil. NACA RM L57F26, 1957.

4. Powell, Robert D., Jr., and Carpenter, Paul J.: Low Tip Mach Number Stall Characteristics and High Tip Mach Number Compressibility Effects on a Helicopter Rotor Having an NACA 0009 Tip Airfoil Section. NACA TN 4355, 1958.

5. Carpenter, Paul J.: Lift and Profile-Drag Characteristics of an NACA 0012 Airfoil Section As Derived From Measured Helicopter-Rotor Hovering Performance. NACA TN 4357, 1958.

6. Abbott, Ira H., von Doenhoff, Albert E., and Stivers, Louis S., Jr.: Summary of Airfoil Data. NACA Rep. 824, 1945. (Supersedes NACA WR L-560).

7. Gessow, Alfred: Effect of Rotor-Blade Twist and Plan-Form Taper on Helicopter Hovering Performance. NACA TN 1542, 1948.

8. Bailey, F. J., Jr.: A Simplified Theoretical Method of Determining the Characteristics of a Lifting Rotor in Forward Flight. NACA Rep. 716, 1941.

9. Graham, Donald J., Nitzberg, Gerald E., and Olson, Robert N.: A Systematic Investigation of Pressure Distributions at High Speeds Over Five Representative NACA Low-Drag and Conventional Airfoil Sections. NACA Rep. 832, 1945.

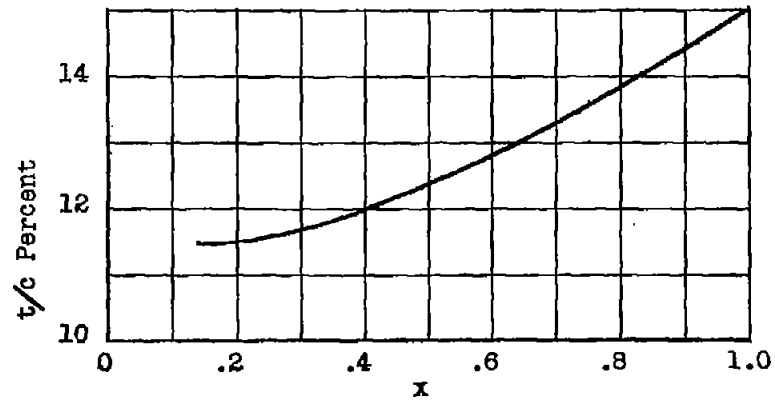

Thickness distribution along span

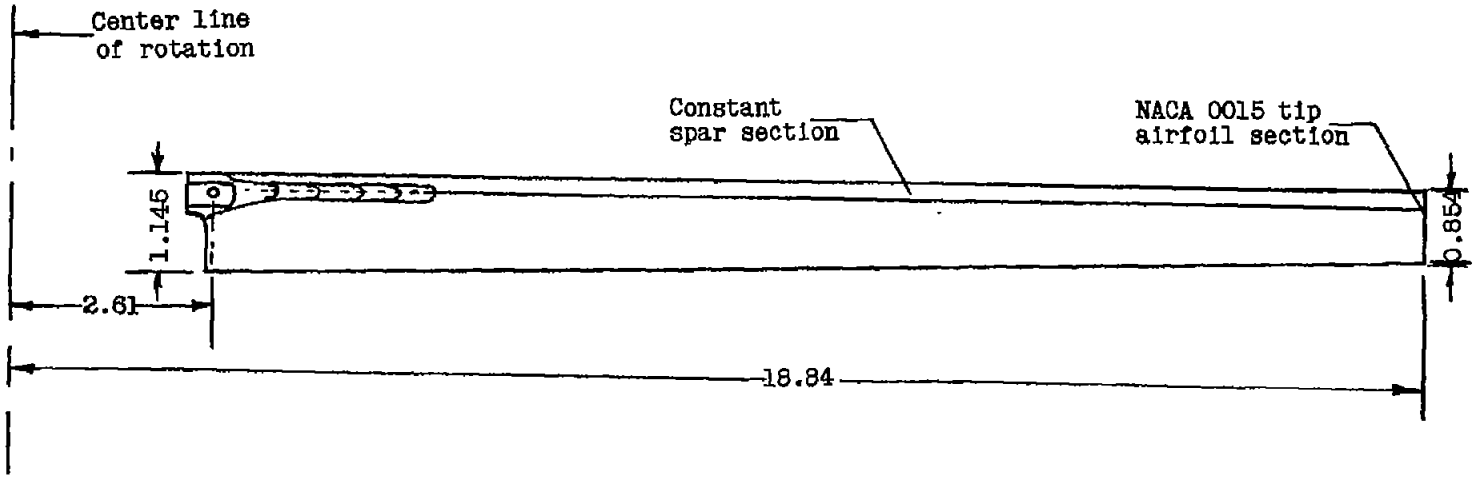

Figure 1.- Sketch of rotor blade having an NACA 0015 tip airfoil section. Chord length tapers from 1.145 feet at the root to 0.854 foot at the tip. $\theta_1 = -5.5^\circ$; $c_e = 0.966$. All dimensions are in feet.

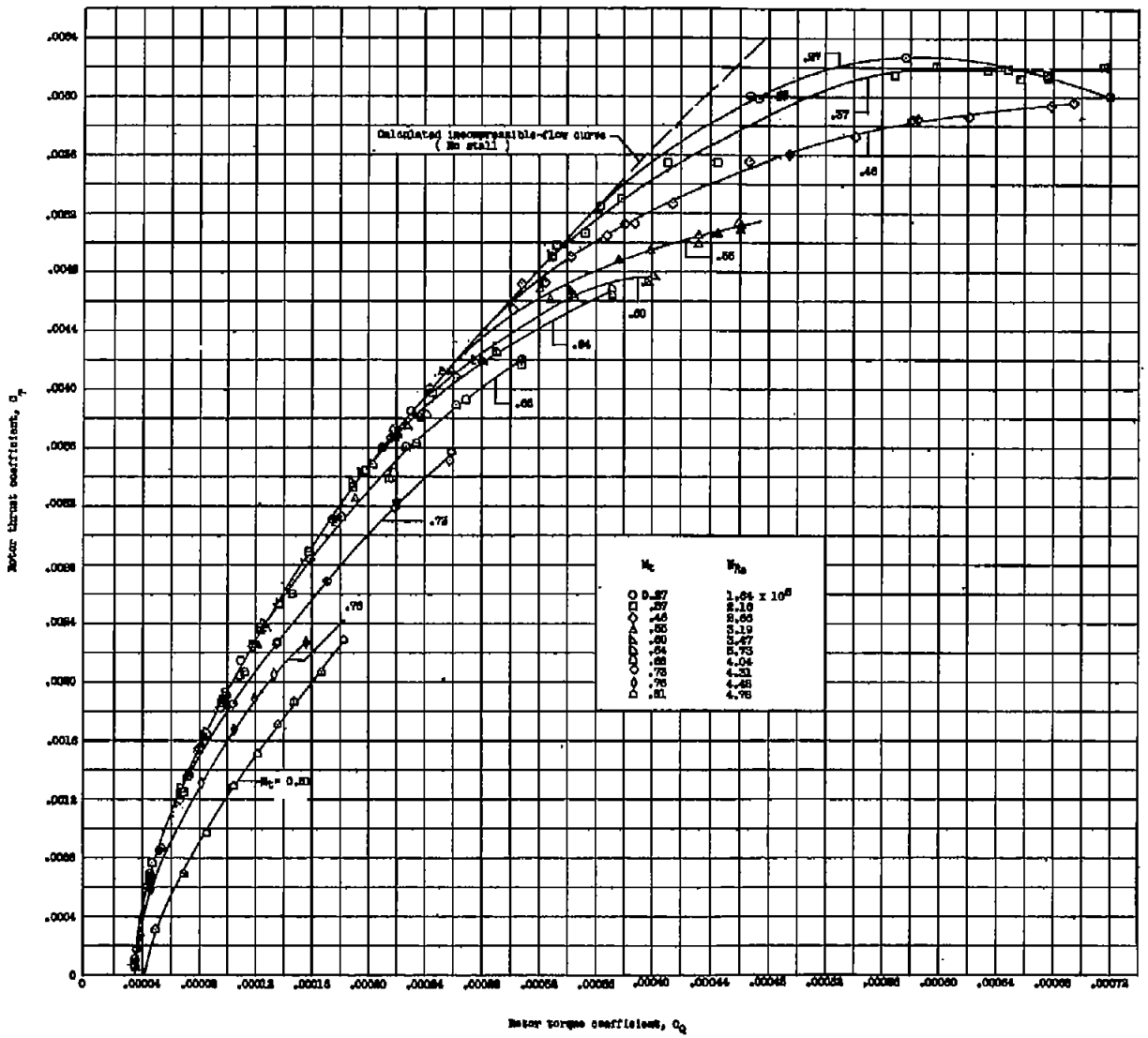

Figure 2.- Hovering performance of smooth rotor blades having NACA 0015 airfoil tip sections. Calculated curve based on $c_{d,o} = 0.0087 - 0.0216\alpha_r + 0.400\alpha_r^2$ and $c_l = 5.73\alpha_r$. $\sigma = 0.033$.

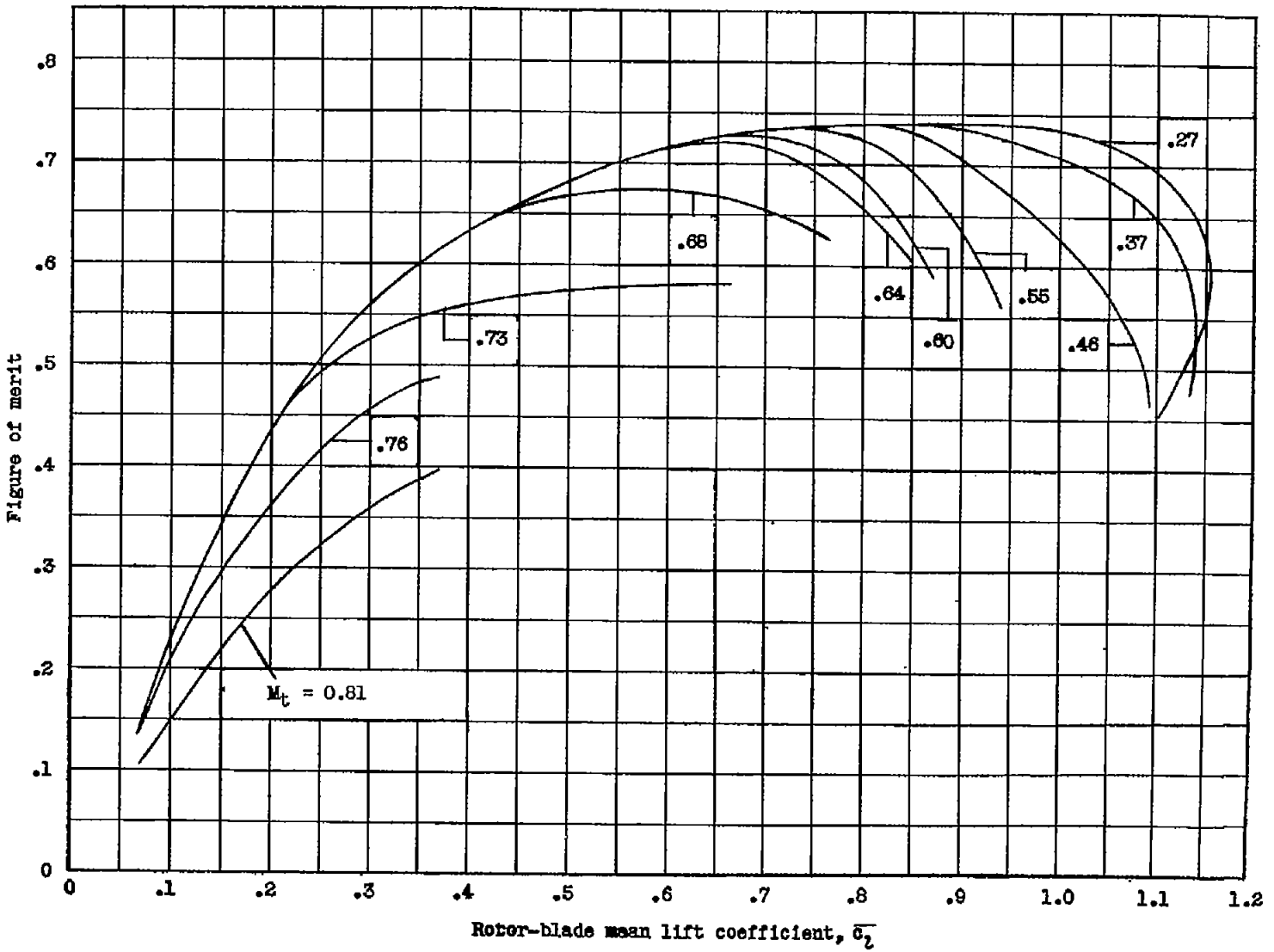

Figure 3.- Effect of tip Mach number on rotor figure of merit for the smooth blade.

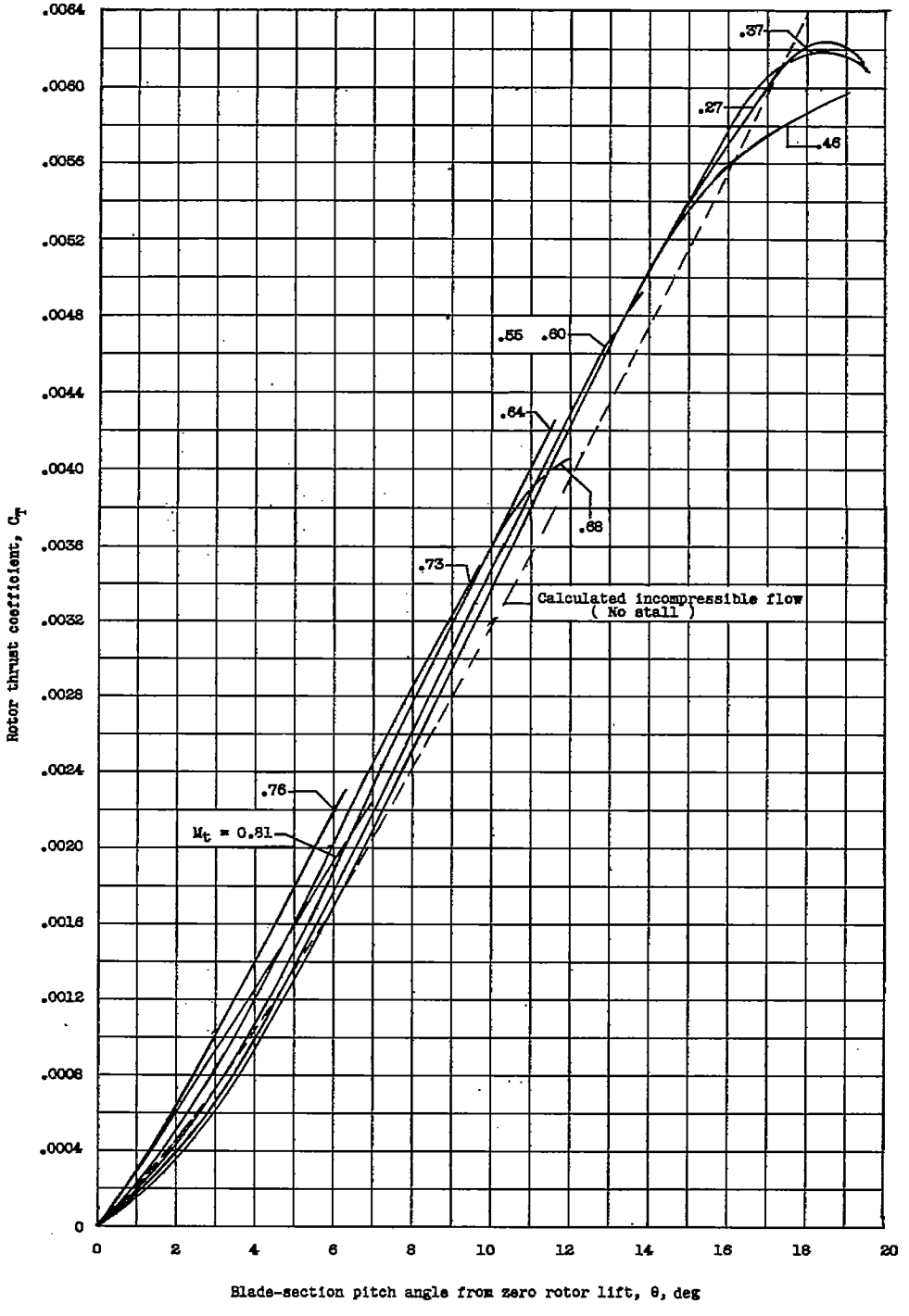

Figure 4.- Variation of rotor thrust coefficient with blade pitch angle for various tip Mach numbers.

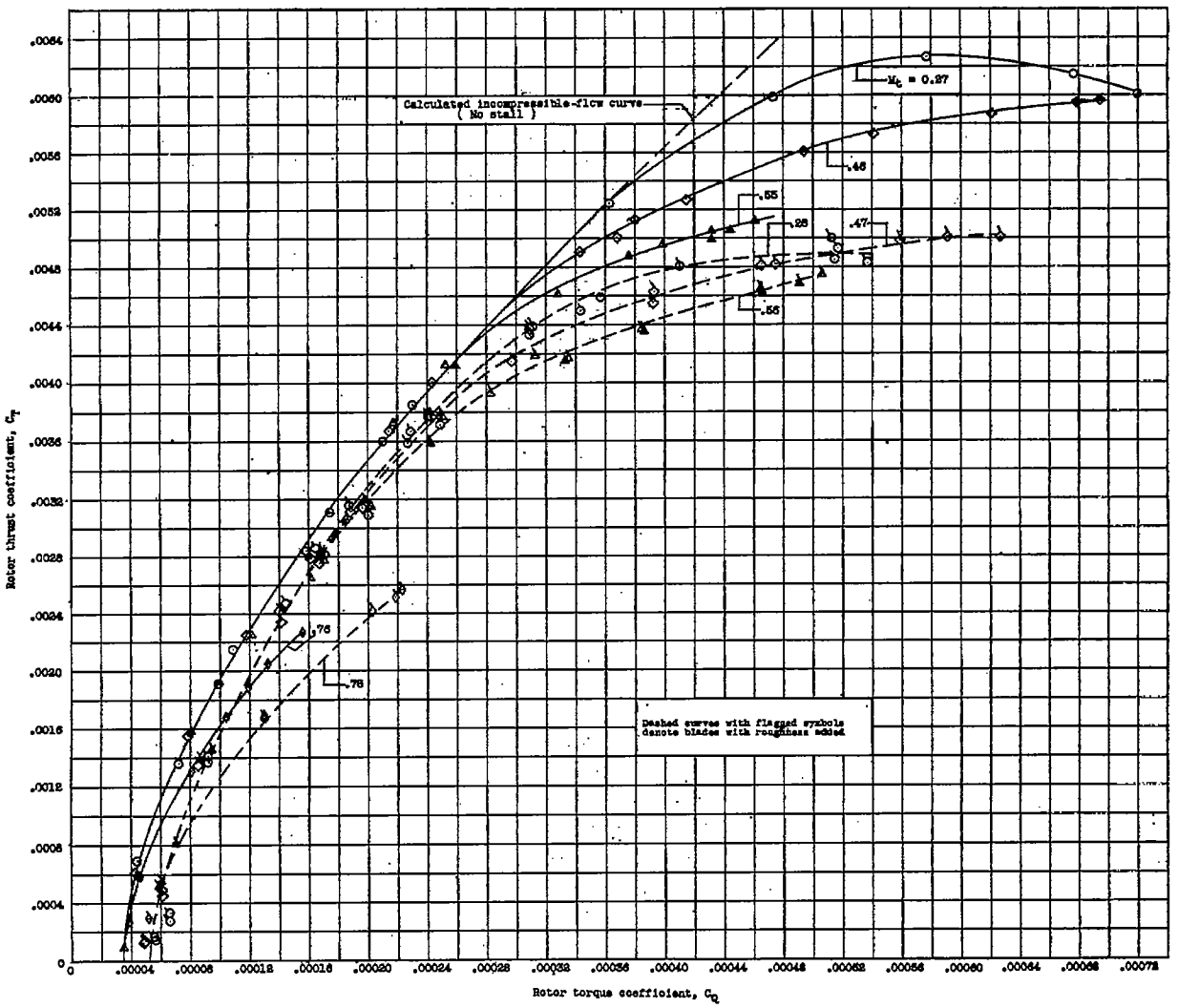

Figure 5.- Effect of blade leading-edge roughness on rotor hovering performance

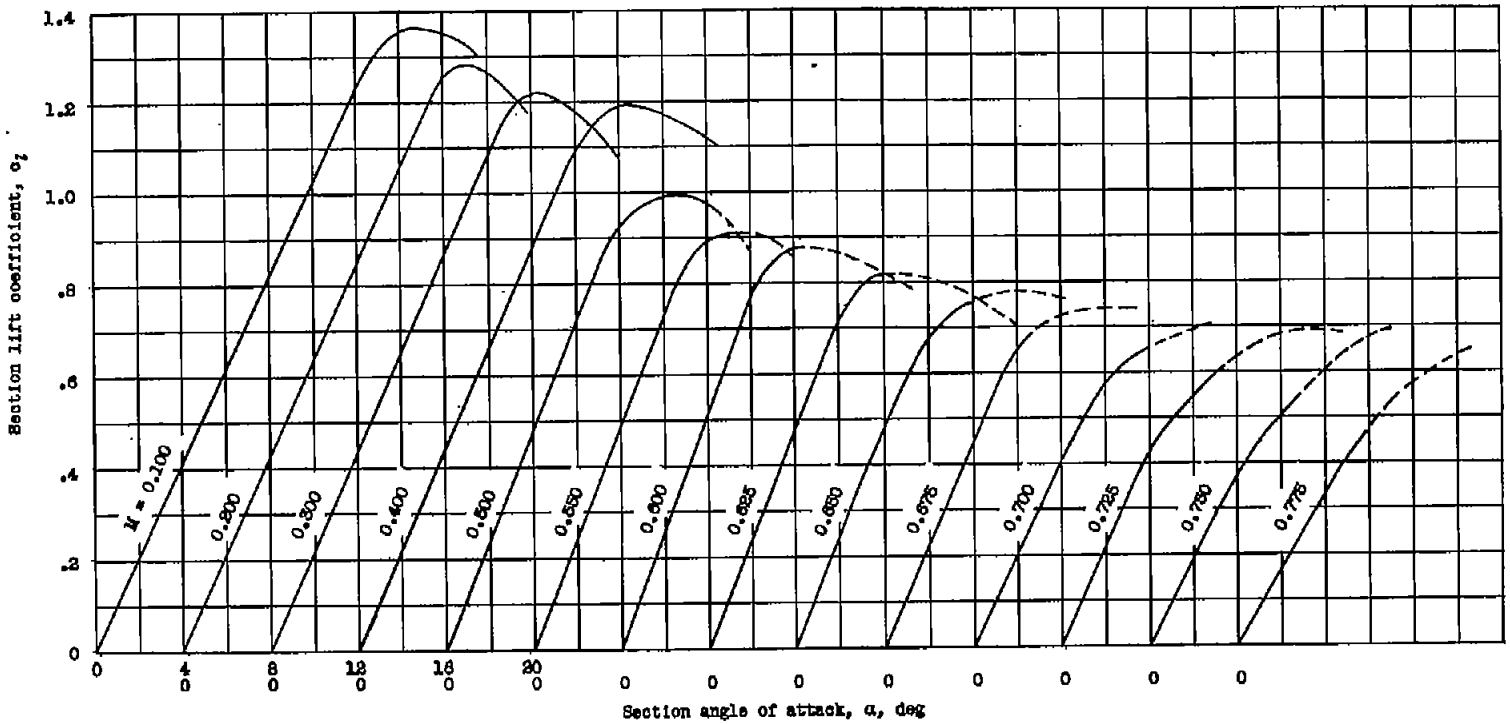

Figure 6.- Variation of synthesized section lift coefficient with angle of attack at various Mach numbers obtained from a rotor having an NACA 0015 tip airfoil section.

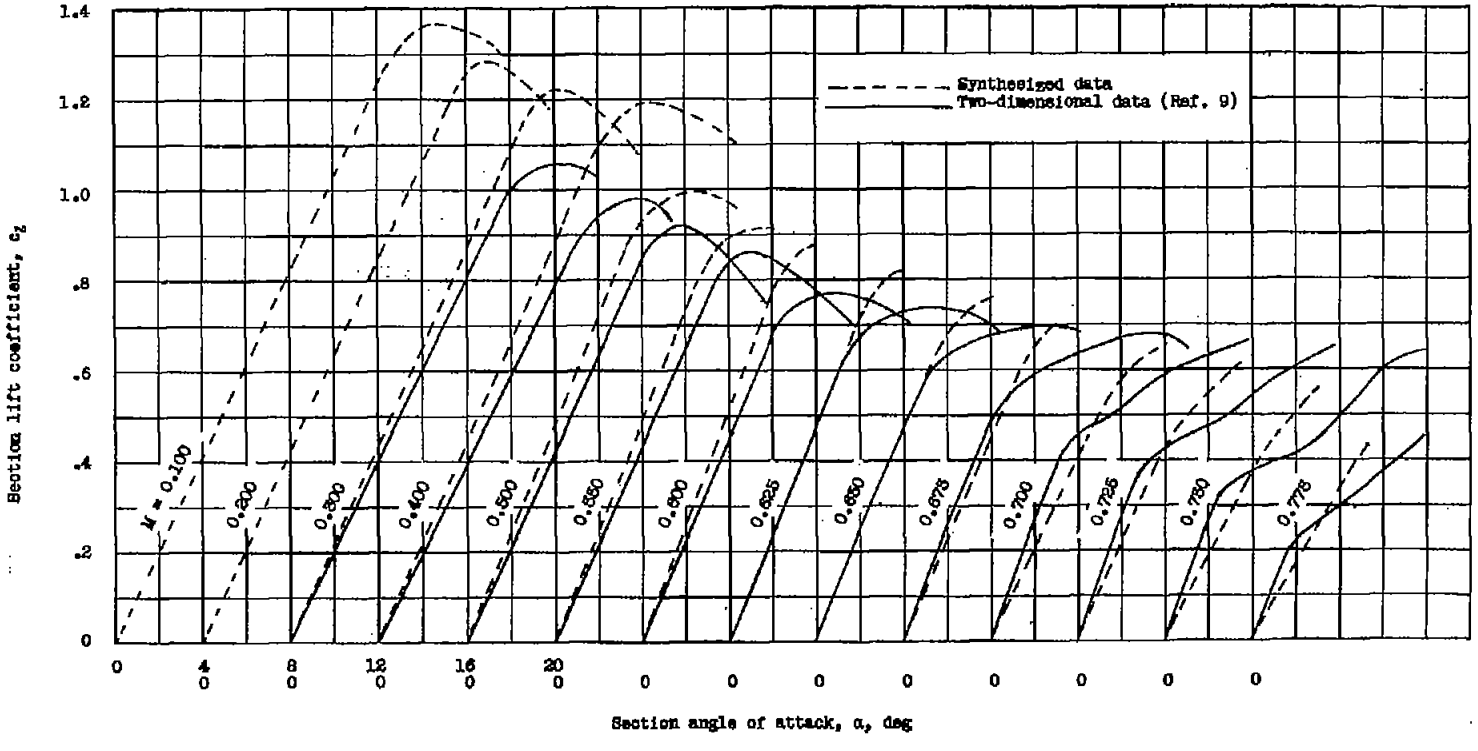

Figure 7.- Comparison of synthesized and two-dimensional section lift coefficient with angle of attack at various Mach numbers.

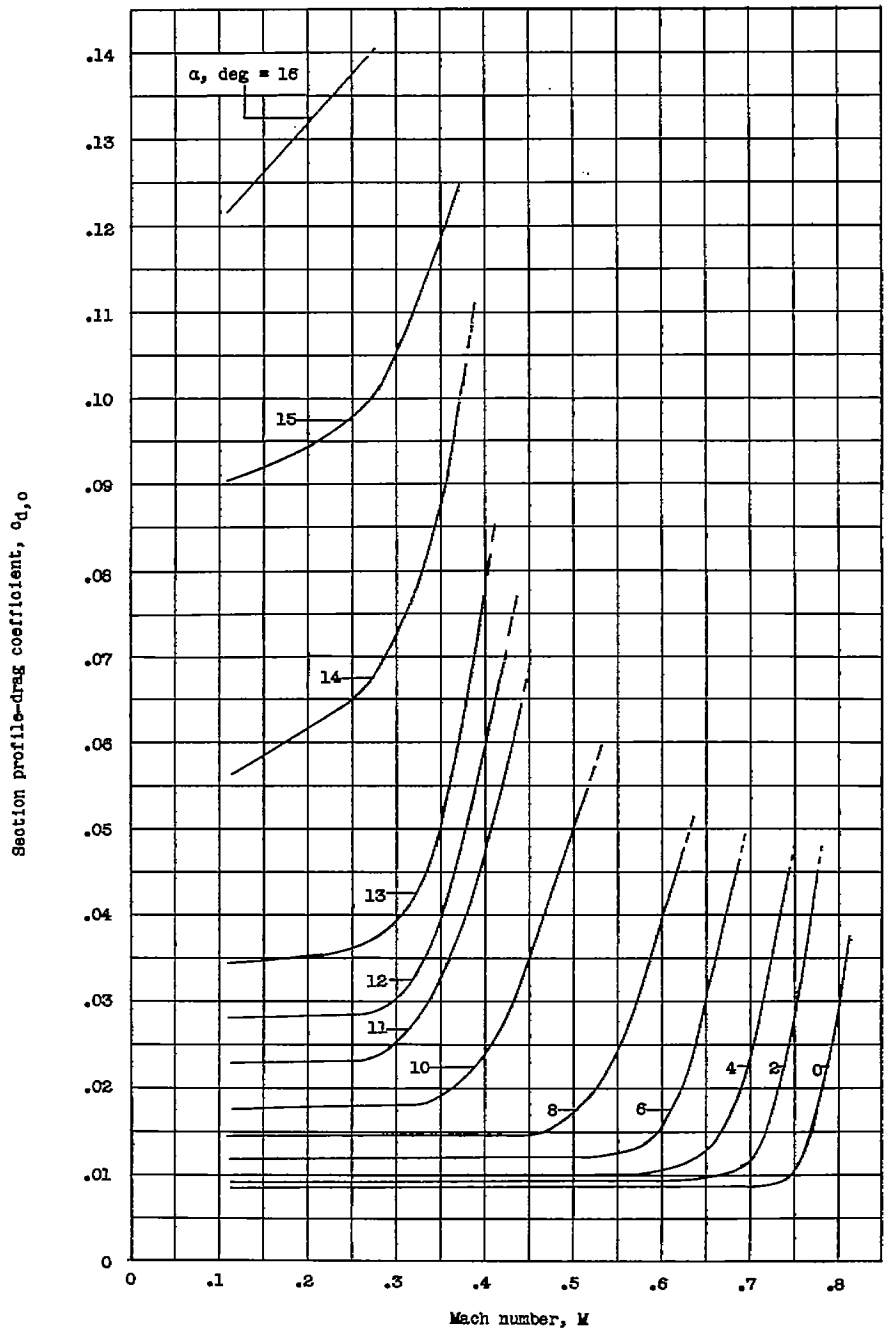

Figure 8.- Variation of synthesized rotor-blade-section profile-drag coefficient with angle of attack at various Mach numbers for an NACA 0015 tip airfoil section. Dashed part of curve represents probable curve but was not verified by experimental data.

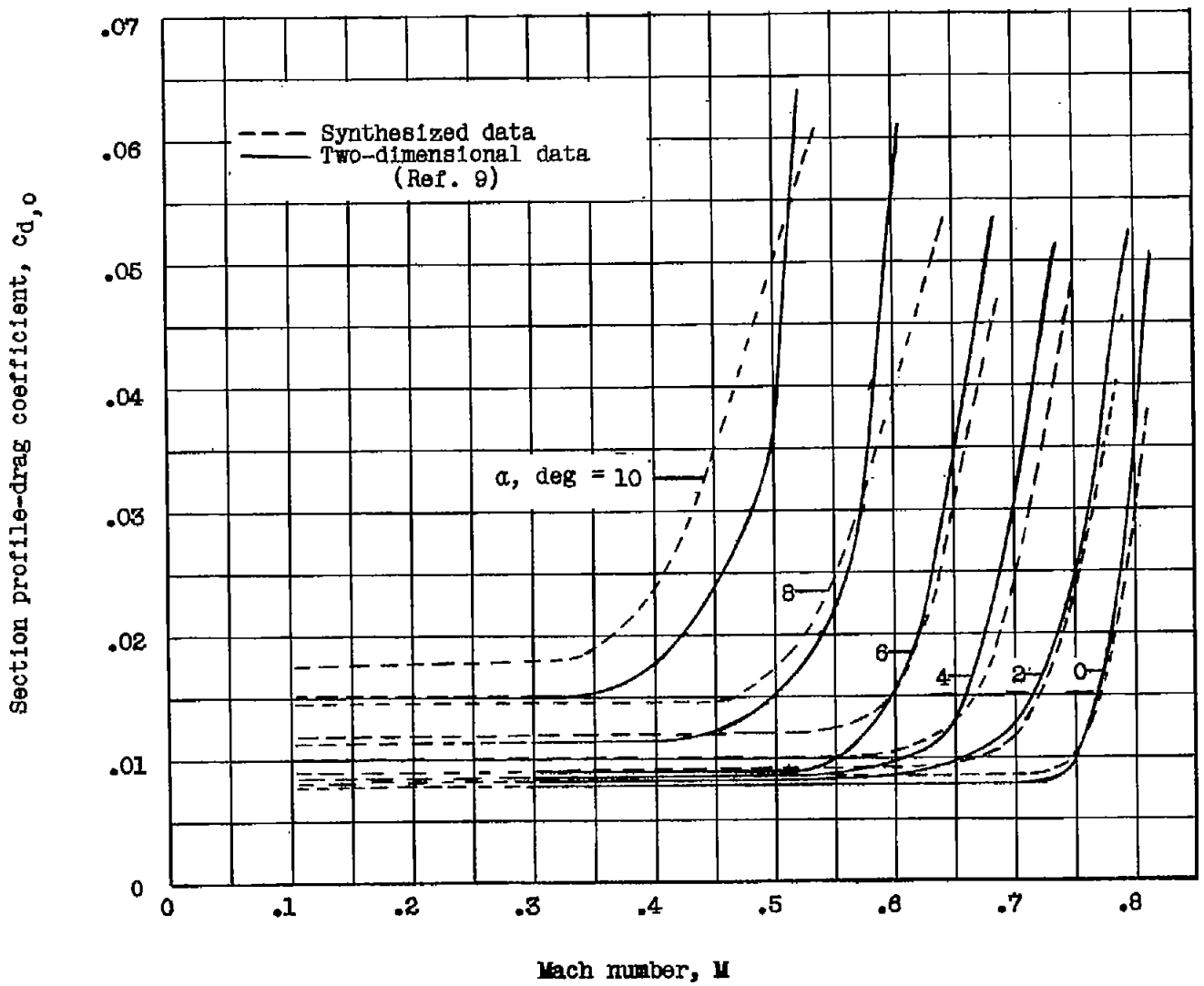

Figure 9.- Comparison of synthesized rotor blade and two-dimensional section profile-drag coefficient with angle of attack at various Mach numbers.

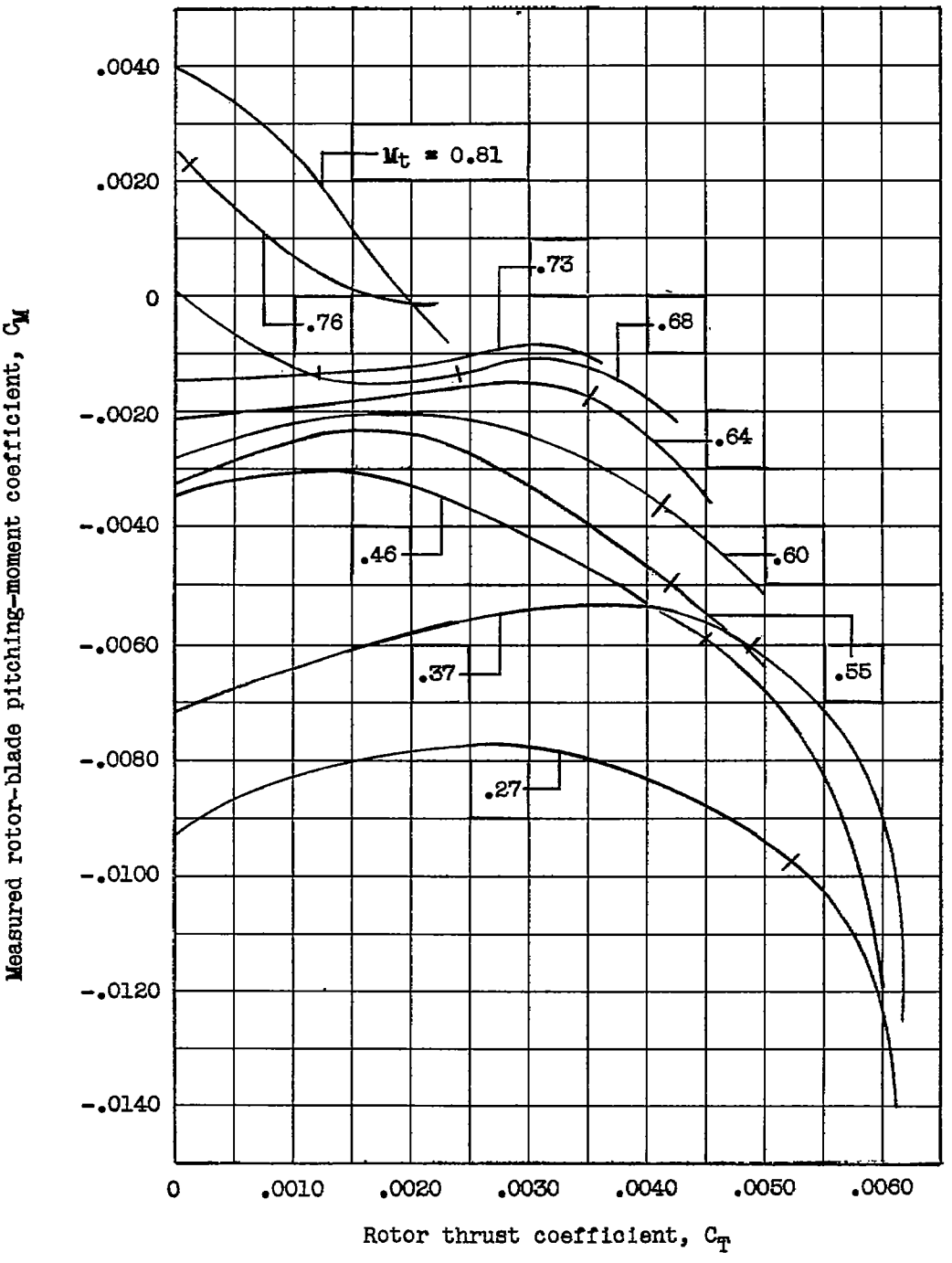

(a) Smooth condition.

Figure 10.- Effect of tip Mach number on the pitching moment of rotor blades having NACA 0015 tip airfoil sections.

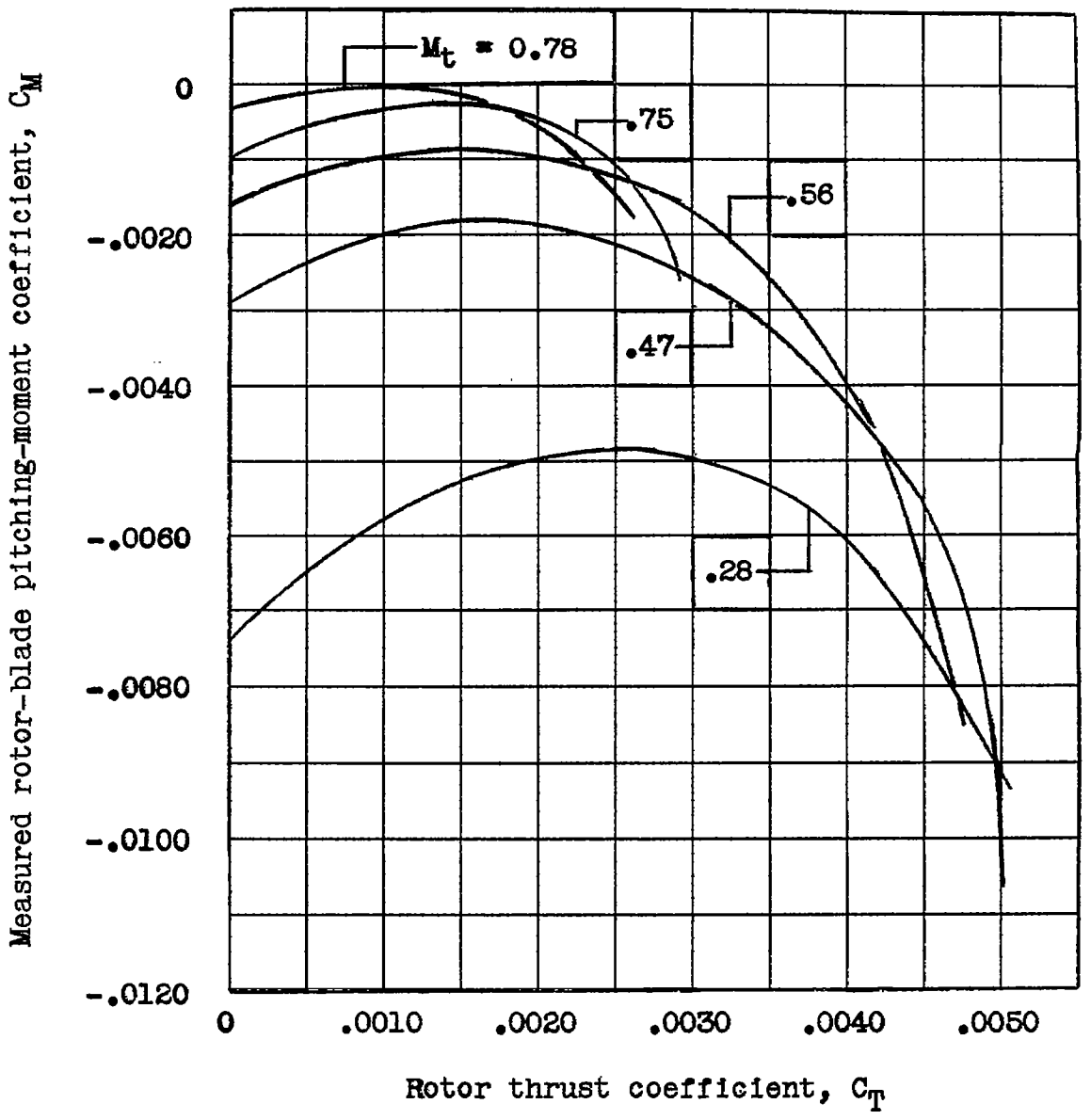

(b) Leading-edge roughness.

Figure 10.- Concluded.

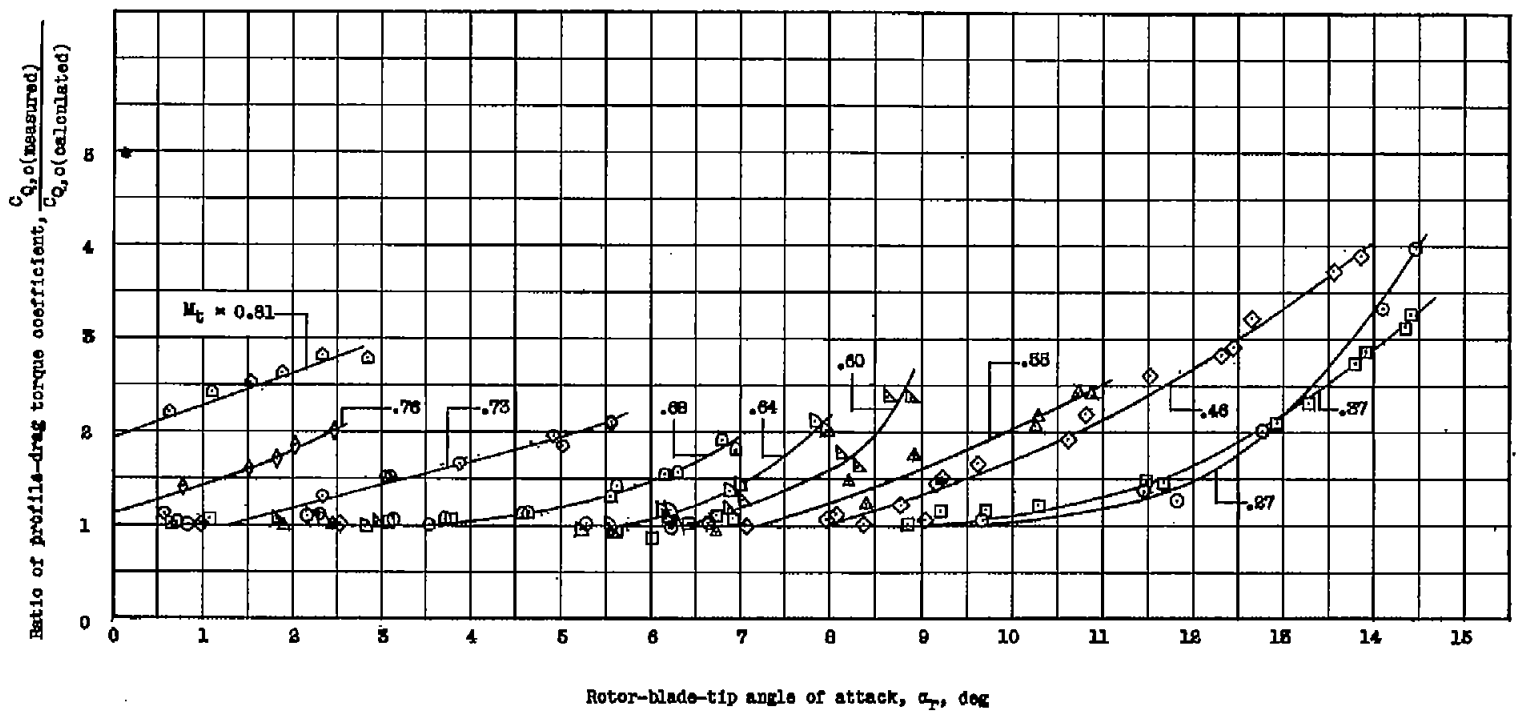

Figure 11.- Effect of tip angle of attack and Mach number on profile-drag torque ratio for smooth rotor blades.

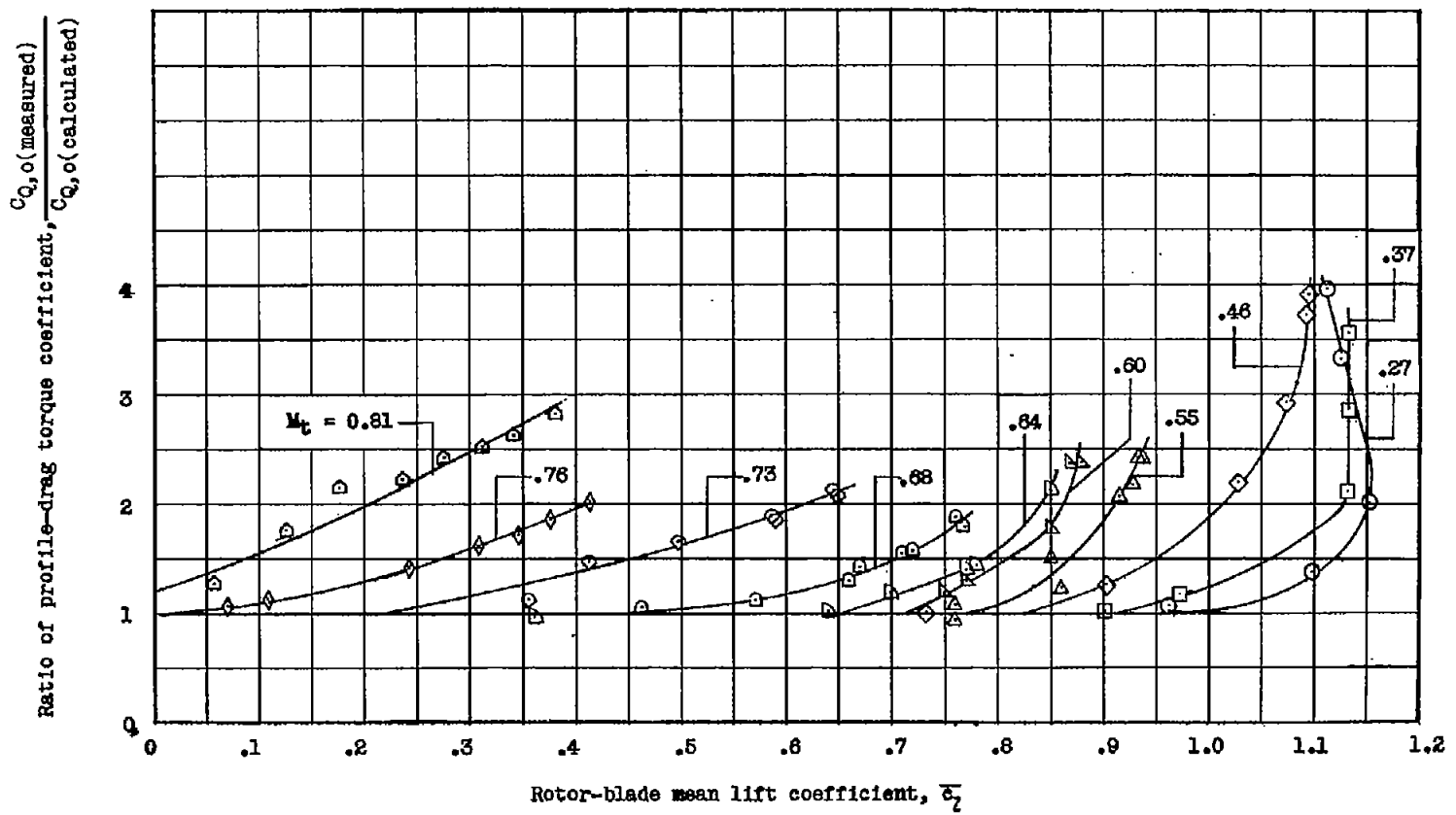

Figure 12.- Effect of Mach number on profile-drag torque ratio for various $\overline{c_l}$ values for smooth rotor blades.

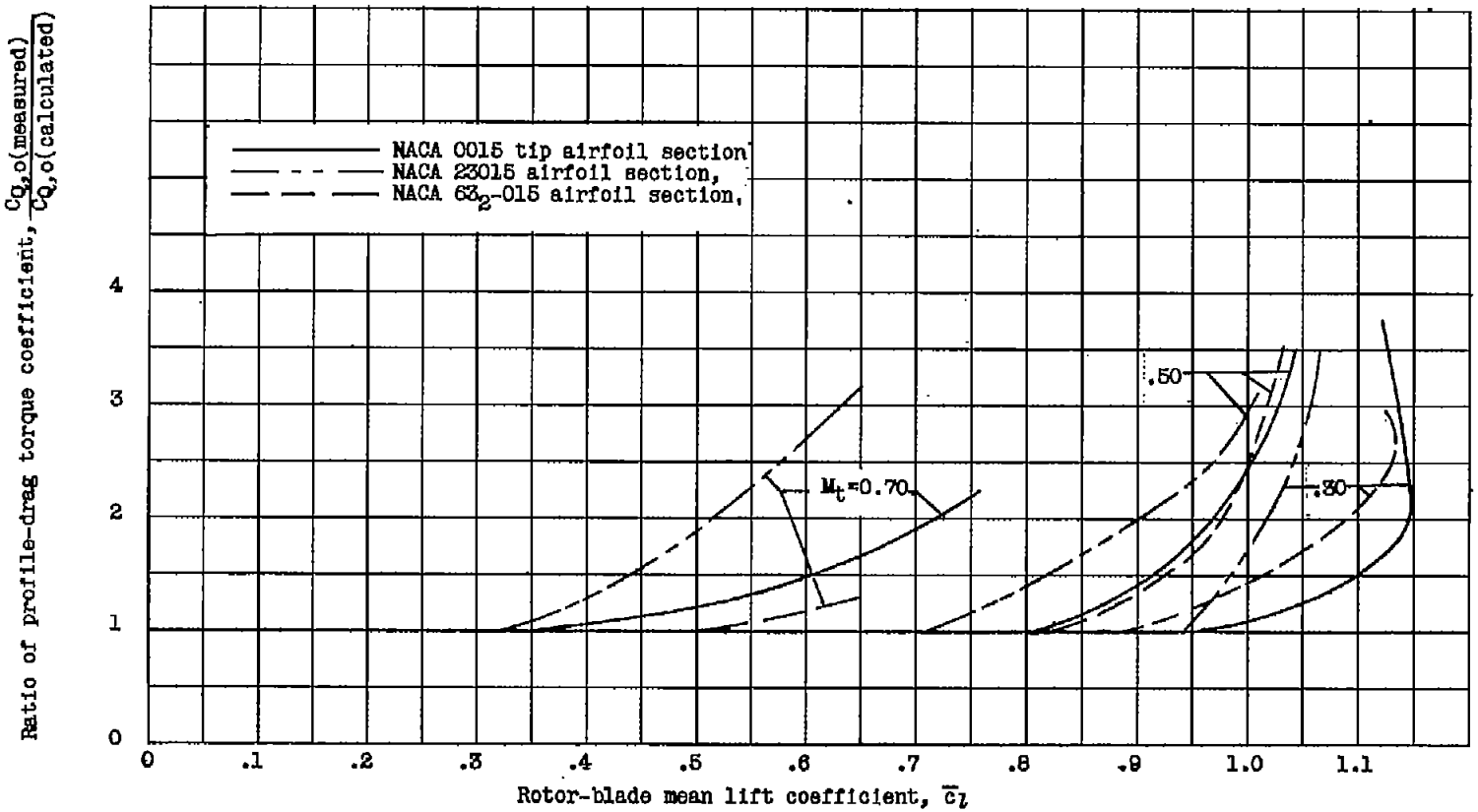

Figure 13.- Comparison of profile-drag torque ratio for three rotors having 15-percent-thick airfoils at various tip Mach numbers.

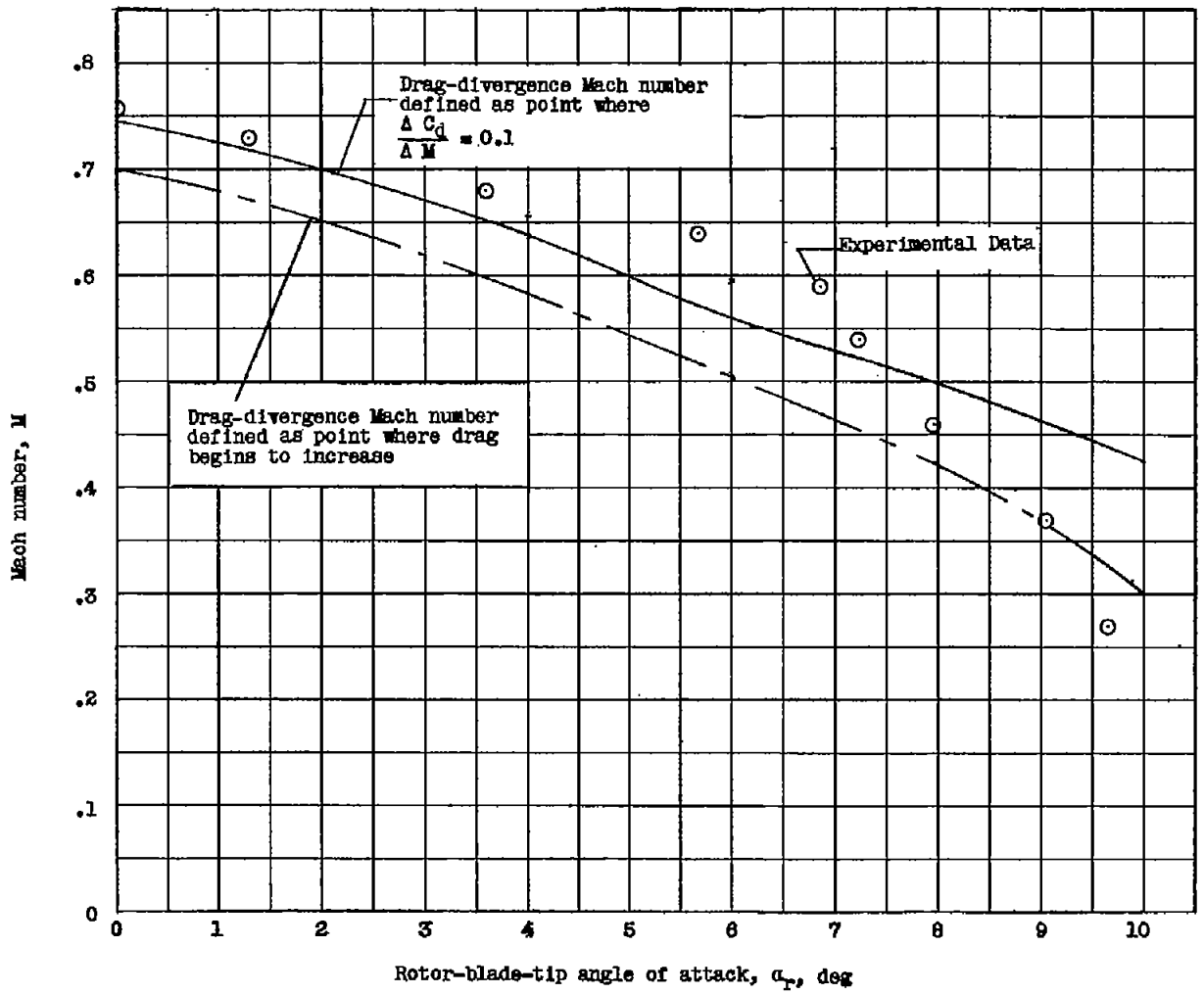

Figure 14.- Comparison of two-dimensional airfoil drag-divergence data with rotor experimental data. The curves are for two-dimensional data for NACA 0015 airfoil section. Symbols represent M_t and α_r at which experimental data from the smooth rotor blade separates from the curve calculated by using the airfoil drag polar $c_{d,o} = 0.0087 - 0.0216\alpha_r + 0.400\alpha_r^2$.